R. & M. No. 2889
(15,232)
A.R.C. Technical Report

MINISTRY OF SUPPLY

AERONAUTICAL RESEARCH COUNCIL
REPORTS AND MEMORANDA

Theoretical Load Distribution on a Wing with a Cylindrical Body at One End

By

J. WEBER, Dr.rer.nat.

LONDON: HER MAJESTY'S STATIONERY OFFICE
1957
PRICE 5*s.* 6*d.* NET

Theoretical Load Distribution on a Wing with a Cylindrical Body at One End

By

J. WEBER, Dr.rer.nat.

COMMUNICATED BY THE PRINCIPAL DIRECTOR OF SCIENTIFIC RESEARCH (AIR), MINISTRY OF SUPPLY

Reports and Memoranda No. 2889*

June, 1952

Summary.—A method is derived for calculating the spanwise load distribution over a lifting wing having a long circular-cylindrical body at one end. The solution is derived for arrangements giving constant induced downwash, but can be generalised to obtain approximate results for other plan-forms including those with sweepback. Charts are given for the case in which the sectional lift slope is constant along the span. The lift distribution over both wing and body can be determined quickly, or the overall load obtained directly.

The results are applicable to the determination of side forces on a fin in combination with the rear fuselage of an aircraft, or of the lift loading on a wing with a weapon or fuel tank at one tip.

1. *Introduction.*—Calculations have been made to determine the spanwise loading on a wing with a cylindrical body at one end only, analogous to the case of a wing with endplate at one end only. The corresponding problem of a wing with cylindrical bodies at both tips has been solved by Hartley[4] (1952) using a similar method to that used here.

The case of the single body and wing may represent a rear fuselage with a fin, particularly if the rear fuselage is a jet-pipe so that it is approximately cylindrical and the diameter is considerable relative to the fin height. It can also represent a wing carrying a single drop-tank or weapon on one tip.

A solution of the problem can be obtained for arrangements where the downwash produced by the trailing vortices is constant along the span. In this case the load distribution can be calculated in the Trefftz-plan far behind the wing. The body is assumed to be of circular cross-section, cylindrical at the wing, and long enough to ensure that the wake behind the system has the shape of the spanwise cross-section through wing and body.

The same method of solution has been used by Nagel and Mangler[1,3] (1938, 1947) for a wing with two endplates, by Rotta[2,3] (1942, 1947) for a single endplate and by Hartley[4] for a wing with two tip tanks. In all these calculations, the assumption of constant induced downwash is made. It has been shown by Hartley[4] and by Küchemann and Kettle[5] (1951) that if the differences obtained by this method are added to the actual span loading of the wing alone, a good approximation is obtained with either unswept or swept wings.

* R.A.E. Report Aero. 2467, received 30th October, 1952.

The present report does not include any comparison with experiment. This will appear elsewhere. The actual calculation procedure to be applied in a practical case is described in section 6.

2. *The Calculation of the Potential Function in the Trefftz-plane.*—The load distribution over the wing and fuselage is proportional to the difference of the potential function on the upper and lower surfaces of the vortex sheet in the Trefftz-plane. To determine the flow in the Trefftz-plane is a two-dimensional problem, which can be solved by conformal transformation, for instance by transforming the wake contour into a circle. The flow in the Trefftz-plane is that around the wake contour moving downwards with constant velocity $v_{z\infty}$. The conformal transformation does not lead to the flow around the circle moving downwards with the velocity $v_{z\infty}$, since the velocities are changed by the transformation. But we can still make use of the conformal transformation, for the flow around the moving wake is the same as the flow around the fixed wake contour in a parallel stream of velocity $-v_{z\infty}$, superimposed upon a parallel flow of velocity $v_{z\infty}$. The conformal transformation transforms the flow around the fixed wake contour into the flow around the fixed circle, for which the potential function is known. Our first task is, therefore, to determine the conformal transformation and thus corresponding points on the circle and the wake contour.

A rectangular co-ordinate system x,y,z is chosen, with x along wind, y spanwise, z positive downwards, with the origin on the body axis. For a thin wing attached to a circular body, a cross-section through the wake in a vertical plane $x = \infty$ (Trefftz-plane) has the shape of a circle $y^2 + z^2 = R^2$ joined to a straight line $-(b + R) < y < -R$, where R is the radius of the body and b the span of the wing outside the body (*see* Fig. 1).

The transformation of the wake contour into the circle is done in two steps. The ζ-plane

$$\zeta = z + iy \qquad \ldots \quad \ldots \quad \ldots \quad \ldots \quad \ldots \quad \ldots \quad (1)$$

is transformed into the ζ_1-plane

$$\zeta_1 = z_1 + iy_1 \qquad \ldots \quad \ldots \quad \ldots \quad \ldots \quad \ldots \quad \ldots \quad (2)$$

by the transformation

$$\zeta_1 = \zeta + \frac{R^2}{\zeta}. \qquad \ldots \quad \ldots \quad \ldots \quad \ldots \quad \ldots \quad \ldots \quad (3)$$

Thus the wing-body configuration of the ζ-plane is transformed into a wing with vertical endplate in the ζ_1-plane (Fig. 1). The height h of the endplate and the wing span b_1 are

$$h = 4R \qquad \ldots \quad \ldots \quad \ldots \quad \ldots \quad \ldots \quad \ldots \quad \ldots \quad (4)$$

$$b_1 = b\,\frac{b + 2R}{b + R}. \qquad \ldots \quad \ldots \quad \ldots \quad \ldots \quad \ldots \quad \ldots \quad (5)$$

The flow around a wing with one endplate has already been treated by Rotta[2]. The ζ_1-plane is transformed into a ζ_2-plane in such a way that the wing with endplate is transformed into a circle of radius R_2. The transformation is

$$\zeta_1 = \sqrt{\left\{\left(\zeta_2 - \frac{R_2^2}{\zeta_2} - 2R_2 i\right)\left(\zeta_2 - \frac{R_2^2}{\zeta_2} - 2R_2 \cos\vartheta_2 \,.\, i\right)\right\}}. \qquad \ldots \quad \ldots \quad (6)$$

Since

$$\zeta_2 = i \,.\, R_2\, e^{i\vartheta} \qquad \ldots \quad \ldots \quad \ldots \quad \ldots \quad \ldots \quad \ldots \quad (7)$$

is the equation for the circle (Fig. 1), the relation between corresponding points on the circle and on wing and endplate in the ζ_1-plane is

$$\zeta_1 = i \,.\, 2R_2 \sqrt{\{(\cos\vartheta - 1)(\cos\vartheta - \cos\vartheta_2)\}} \,. \quad .. \quad .. \quad .. \quad (8)$$

$\vartheta = 0$ corresponds to the point $y = R$, $z = 0$ on the body; $\vartheta = \pm\vartheta_2$ to the junction of wing and endplate, *i.e.*, the junction of wing and body. The ends of the endplate $\zeta = \mp \frac{1}{2}h$, i.e., the top and bottom of the body, correspond to the angle $\pm\vartheta_1$, for which

$$\cos\vartheta_1 = \tfrac{1}{2}(1 + \cos\vartheta_2) \,. \quad .. \quad .. \quad .. \quad .. \quad .. \quad (9)$$

The height of the endplate is

$$h = 2R_2(1 - \cos\vartheta_2) \,. \quad .. \quad .. \quad .. \quad .. \quad .. \quad (10)$$

The point $\zeta_1 = 0 - ib_1$ corresponds to $\vartheta = \pi$, so that

$$b_1 = R_2 \,.\, 2\sqrt{2}\sqrt{(1 + \cos\vartheta_2)} \,. \quad .. \quad .. \quad .. \quad .. \quad (11)$$

The square root $\sqrt{\{(\cos\vartheta - 1)(\cos\vartheta - \cos\vartheta_2)\}}$ must be taken with the positive sign for $0 < \vartheta < \vartheta_2$ and with the negative sign for $\vartheta_2 < \vartheta < \pi$. Equations (4), (5) together with equations (10), (11) give two relations for the unknown quantities ϑ_2 and R_2:

$$\frac{h}{b_1} = \frac{1 - \cos\vartheta_2}{\sqrt{2}\sqrt{(1 + \cos\vartheta_2)}} = \frac{4R(b + R)}{b(b + 2R)} \quad .. \quad .. \quad .. \quad (12)$$

$$R_2 = \frac{2R}{1 - \cos\vartheta_2} \,. \quad .. \quad .. \quad .. \quad (13)$$

The points on the circle $0 \leqslant |\vartheta| \leqslant \vartheta_2$ are related to the points on the body cross-section in the ζ-plane by the equation

$$\frac{y}{R} = \sqrt{\left\{1 - \left(\frac{z}{R}\right)^2\right\}} = \sqrt{\left\{1 - \frac{1}{4}\left(\frac{z_1}{R}\right)^2\right\}}$$

$$= \sqrt{\left\{1 - \frac{1}{4}\cdot\frac{4R_2^2}{R^2}(1 - \cos\vartheta)(\cos\vartheta - \cos\vartheta_2)\right\}}$$

$$\frac{y}{R} = +\sqrt{\left\{1 - \frac{4}{(1 - \cos\vartheta_2)^2}(1 - \cos\vartheta)(\cos\vartheta - \cos\vartheta_2)\right\}} \text{ for } 0 \leqslant |\vartheta| \leqslant \vartheta_1 \quad .. \quad (14)$$

$$\frac{y}{R} = -\sqrt{\left\{1 - \frac{4}{(1 - \cos\vartheta_2)^2}(1 - \cos\vartheta)(\cos\vartheta - \cos\vartheta_2)\right\}} \text{ for } \vartheta_1 \leqslant |\vartheta| \leqslant \vartheta_2 \,. \quad (15)$$

The points on the circle $\vartheta_2 \leqslant |\vartheta| \leqslant \pi$ are related to the points on the wing section in the ζ-plane by the equation:

$$\frac{y}{R} = \frac{1}{2}\frac{y_1}{R} + \sqrt{\left\{1 + \left(\frac{1}{2}\frac{y_1}{R}\right)^2\right\}}$$

$$= -\left[\frac{2}{1 - \cos\vartheta_2}\sqrt{\{(1 - \cos\vartheta)(\cos\vartheta_2 - \cos\vartheta)\}}\right.$$

$$\left. + \sqrt{\left\{1 + \frac{4}{(1 - \cos\vartheta_2)^2}(1 - \cos\vartheta)(\cos\vartheta_2 - \cos\vartheta)\right\}}\right] \,. \quad .. \quad .. \quad .. \quad (16)$$

The potential function for the circle in a parallel flow with the velocity $-v_{z\infty}$ is

$$\phi_1 = 2R_2 v_{z\infty} \sin\vartheta \,, \qquad \ldots \qquad (17)$$

for points on the circle. This is also the potential function for the flow around the fixed wake contour. The potential of the parallel flow is

$$\phi_2 = v_{z\infty} z \,. \qquad \ldots \qquad (18)$$

Hence, the potential function for the moving wake contour in the Trefftz-plane is

$$\phi = \phi_1 + \phi_2 = v_{z\infty}\left[\frac{4R}{1-\cos\vartheta_2}\sin\vartheta + z\right] \qquad \ldots \qquad (19)$$

where equations (14), (15) and (16) give the relation between y and ϑ ; ϑ_2 is determined by the ratio R/b according to equation (12).

3. *The Calculation of the Load Distribution and the Overall Lift Coefficient.*—The local lift coefficient on the wing and body is related to the difference of the potential function on the upper and lower surfaces of the vortex sheet in the Trefftz-plane by

$$C_L = \frac{2}{cV_0}(\phi_{US} - \phi_{LS}) \qquad \ldots \qquad (20)$$

where c is the local chord, used as reference chord for the local lift coefficient C_L , and V_0 is the velocity of the main flow. This relation can be justified as follows. In linear theory, the pressure coefficient C_p at any point is given by

$$C_p = -2\frac{v_x}{V_0} = -\frac{2}{V_0}\frac{\partial\phi}{\partial x} \,.$$

The lift coefficient is equal to the integrated difference of the pressure coefficients on upper and lower surface:

$$C_L = \int_{-\infty}^{+\infty} -\Delta C_p \, d(x/c) \,.$$

From equations (19) and (20),

$$C_L \,.\, c = 4\frac{v_{z\infty}}{V_0}\left[\frac{4R}{1-\cos\vartheta_2}\sin\vartheta - \sqrt{(R^2-y^2)}\right] \qquad \ldots \qquad (21)$$

for $|y| < R$, i.e., for the body

and

$$C_L \,.\, c = 4\frac{v_{z\infty}}{V_0}\frac{4R}{1-\cos\vartheta_2}\sin\vartheta \qquad \ldots \qquad (22)$$

for $|y| > R$, i.e., for the wing

since ϑ is positive and $z = \sqrt{(R^2-y^2)}$ is negative on the upper surface of wing and body.

The coefficient of the overall lift over the wing is obtained by integration; $\bar{C}_{LW}$ is referred to the wing area $b\bar{c}$, where $\bar{c}$ is the mean wing chord. We find

$$\bar{C}_{LW} \cdot \bar{c} = \int_{-\frac{b+R}{b}}^{-R/b} C_L \cdot c \, d\left(\frac{y}{b}\right)$$

which gives

$$\bar{C}_{LW} = \frac{v_{z\infty}}{V_0} \frac{b}{\bar{c}} \frac{16(R/b)^2}{1 - \cos\vartheta_2} \int_{-\left(\frac{b}{R}+1\right)}^{-1} \sin\vartheta \, d\left(\frac{y}{R}\right) \quad .. \quad .. \quad .. \quad (23)$$

or,

$$\bar{C}_{LW} = \frac{v_{z\infty}}{V_0} A \cdot J_W \quad .. \quad .. \quad .. \quad .. \quad .. \quad .. \quad .. \quad (24)$$

where A is the aspect ratio of the wing and

$$J_W = \frac{16(R/b)^2}{1 - \cos\vartheta_2} \int_{-\left(\frac{b}{R}+1\right)}^{-1} \sin\vartheta \, d\left(\frac{y}{R}\right) \quad .. \quad .. \quad .. \quad .. \quad (25)$$

is a function only of R/b.

The overall lift over the body, also referred to the wing area $b\bar{c}$, is

$$\bar{C}_{LB} \cdot \bar{c} = \int_{-R/b}^{+R/b} C_L \cdot c \, d\left(\frac{y}{b}\right)$$

or,

$$\bar{C}_{LB} = \frac{v_{z\infty}}{V_0} A \cdot J_B \quad .. \quad .. \quad .. \quad .. \quad .. \quad .. \quad .. \quad (26)$$

with

$$J_B = \frac{16(R/b)^2}{1 - \cos\vartheta_2} \int_{-1}^{+1} \sin\vartheta \, d\left(\frac{y}{R}\right) - 4\left(\frac{R}{b}\right)^2 \int_{-1}^{+1} \sqrt{\left\{1 - \left(\frac{y}{R}\right)^2\right\}} \, d\left(\frac{y}{R}\right)$$

$$= \frac{16(R/b)^2}{1 - \cos\vartheta_2} \int_{-1}^{+1} \sin\vartheta \, d\left(\frac{y}{R}\right) - 2\pi\left(\frac{R}{b}\right)^2 \quad .. \quad .. \quad .. \quad .. \quad .. \quad (27)$$

J_B too is dependent only on R/b. The ratio between the lift on the body and the lift on the wing is

$$\frac{\bar{C}_{LB}}{\bar{C}_{LW}} = \frac{J_B}{J_W} . \quad .. \quad .. \quad .. \quad .. \quad .. \quad .. \quad (28)$$

Thus we find that the ratio $\bar{C}_{LB}/\bar{C}_{LW}$ between the individual load contributions depends only on the ratio R/b between body radius and wing span. Values of J_W and $\bar{C}_{LB}/\bar{C}_{LW}$ are plotted in Figs. 2 and 3.

The shape of the spanwise load distribution depends only on R/b. By equations (21), (22) and (23),

$$\frac{C_L c}{\bar{C}_{LW} \bar{c}} = \frac{1}{R/b} \frac{\sin\vartheta}{\int_{-\left(\frac{b}{R}+1\right)}^{-1} \sin\vartheta \, d\left(\frac{y}{R}\right)} \quad \text{for the wing,} \quad |y| > R \quad .. \quad .. \quad .. \quad (29)$$

and

$$\frac{C_L c}{\bar{C}_{LW} \bar{c}} = \frac{1}{R/b} \frac{\sin\vartheta - \frac{1 - \cos\vartheta_2}{4} \sqrt{\left\{1 - \left(\frac{y}{R}\right)^2\right\}}}{\int_{-\left(\frac{b}{R}+1\right)}^{-1} \sin\vartheta \, d\left(\frac{y}{R}\right)} \quad \text{for the body,} \quad |y| < R . \quad (30)$$

Again equations (14), (15) and (16) give the relation between y and ϑ. For the practical range of values of R/b, the spanwise load distributions have been calculated and the results plotted in Fig. 4. Fig. 4 shows that with bodies of small diameter the shape of the load distribution already differs considerably from the elliptic distribution of the wing alone; there is a large increase of wing lift near the wing-body junction. The determination of the shape of the load distribution for any R/b value is easily done from Figs. 5 and 6; in Fig. 6 the load on the body is referred to that in the wing-body junction. To find the actual load the coefficient of the overall wing-load is needed; this is determined by equations (24) and (25) except for the factor $v_{z\infty}/V_0$. The next step in the calculation is therefore to determine $v_{z\infty}/V_0$ in terms of known quantities.

4. *The Calculation of the Downwash Velocity.*—The value of the downwash depends on the aspect ratio of the wing, the sectional lift slope a, and the ratio R/b. The local lift is equal to a multiplied by the effective incidence, which is equal to the geometric incidence α of the wing, increased by the additional upwash $\Delta\alpha_B$ produced by the flow around the isolated body and reduced by the induced incidence α_i.

As has been explained in detail in Ref. 6 for the case of a body with symmetrically attached wing and zero wing-body angle:

$$\Delta\alpha_B = \alpha\frac{1}{(y/R)^2}. \qquad \ldots\ldots\ldots\ldots\ldots\ldots \quad (31)$$

The incidence α_i which the trailing vortices induce at the wing can be taken as proportional to the downwash far downstream:

$$\alpha_i = \frac{v_z}{V_0} = \frac{\omega}{2}\frac{v_{z\infty}}{V_0}. \qquad \ldots\ldots\ldots\ldots\ldots\ldots \quad (32)$$

The value of ω depends mainly on the aspect ratio of the wing. $\omega = 1$ for wings of large aspect ratio and $\omega = 2$ for wings with $A \to 0$. A method for calculating ω has been derived by Küchemann[7] (1952) for isolated wings, and the relation from which ω can be determined is given in section 6.

It is not strictly correct to apply this relation to our case where the vorticity is essentially composed of two parts, the first determined by the geometric incidence α and the other by $\Delta\alpha_B$. The first part is similar to that of a wing alone, but with the second one the bound vorticity is concentrated near the leading edge and is changing rapidly spanwise. Thus as for very small aspect ratio wings the downwash produced by the chordwise vortices and the trailing vortices is the same on the wing as far downstream in the wake. This means that different values for the 'effective aspect ratio' should be taken in determining ω, so that the value of ω is nearly 2 for the part of $v_{z\infty}$ produced by the second part of the vorticity and $\omega < 2$ for the first part. It has been found possible to distinguish between these different values of ω for wings attached symmetrically to a body (*see* Ref. 6) but since in the present case there is no possibility of splitting $v_{z\infty}$ into the corresponding parts and since the second part is only a correction term to the first part, we take the same ω for both.

Thus we obtain

$$\frac{C_L(y)}{\alpha} = a(y)\left[1 + \frac{1}{(y/R)^2} - \frac{\omega}{2}\frac{v_{z\infty}/V_0}{\alpha}\right]. \qquad \ldots\ldots\ldots \quad (33)$$

The sectional lift slope is a function of A, and for swept wings, of the angle of sweep and the spanwise position, *see* Refs. 7, 8. A relation from which a can be found is also given in section 6.

The condition that the arrangement considered gives constant induced downwash implies that the wing must have a certain plan-form*. This plan-form can be found by combining equations (22) and (33):

$$\frac{c(y)}{R} = \frac{v_{z\infty}/V_0}{\alpha} \cdot \frac{16}{1 - \cos\vartheta_2} \cdot \frac{1}{a(y)} \cdot \frac{\sin\vartheta}{1 + \left(\frac{1}{y/R}\right)^2 - \frac{\omega}{2}\frac{v_{z\infty}/V_0}{\alpha}} \cdot \quad \ldots \quad \ldots \quad (34)$$

Integrating $c(y)$ along the span,

$$\int_{-\left(\frac{b}{R}+1\right)}^{-1} \frac{c(y)}{R}\, d\left(\frac{y}{R}\right) = \frac{\bar{c} \cdot b}{R^2} = \frac{1}{A} \cdot \frac{1}{(R/b)^2} \quad \ldots \quad \ldots \quad \ldots \quad \ldots \quad (35)$$

gives the required relationship between $\frac{v_{z\infty}/V_0}{\alpha}$ and A, a, ω, R/b:

$$\frac{1}{A}\frac{1}{(R/b)^2} = \frac{v_{z\infty}/V_0}{\alpha} \cdot \frac{16}{1 - \cos\vartheta_2} \int_{-\left(\frac{b}{R}+1\right)}^{-1} \frac{\sin\vartheta}{a(y)\left[1 + \frac{1}{(y/R)^2} - \frac{\omega}{2}\frac{v_{z\infty}/V_0}{\alpha}\right]}\, d\left(\frac{y}{R}\right). \quad \ldots \quad (36)$$

For constant $a(y) = a$:

$$\frac{\omega a}{A} = \frac{\omega}{2}\frac{v_{z\infty}/V_0}{\alpha}\left(\frac{R}{b}\right)^2 \frac{32}{1 - \cos\vartheta_2} \int_{-\left(\frac{b}{R}+1\right)}^{-1} \frac{\sin\vartheta}{1 + \frac{1}{(y/R)^2} - \frac{\omega}{2}\frac{v_{z\infty}/V_0}{\alpha}}\, d\left(\frac{y}{R}\right) \quad \ldots \quad (37)$$

which shows that the term $\omega a/A$ is a function of R/b and $\alpha_i/\alpha = \frac{1}{2}\omega\,(v_{z\infty}/V_0)/\alpha$. Though we cannot express α_i/α explicitly as a function of $\omega a/A$ and R/b we can determine values of the integral in equation (37) graphically and thus prepare a diagram from which values of α_i/α can be read. Such a diagram, which covers most practical cases, is given in Fig. 7.

If a spanwise variation of a is to be taken into account, α_i/α has to be worked out by an iterative process. Since the spanwise variation of a is a function of the distances from the wing-body junction and the wing tip, measured in terms of the local chord $c(y)$, this must be determined from equation (34) assuming a first approximation for $v_{z\infty}/V_0$ and $a(y)$. Then with a known $c(y)$, new $a(y)$ values can be found. Determining the integral of equation (36) will then yield the second approximation to $v_{z\infty}/V_0$.

We restrict ourselves in the following to constant values of a. The error involved is not necessarily great (*see* also Ref. 4) and will be small as far as the overall values of the lift are concerned. For swept wings we take the lift slope of the 'sheared' part of the wing.

The uncertainty about the value of ω, discussed above, will also affect the load distribution across the body, which acts as a lifting surface of small aspect ratio. Hence, $\omega_B = 2$ seems appropriate for the body in most cases. It is not possible to take account of this fact if we retain the restriction to constant induced downwash, *i.e.*, assume that the wing and body wakes move downwards with the same speed, so that a spanwise section through the wake has the same shape as a spanwise section through the actual wing and body. In reality the downwash distribution in the wind direction behind the wing will be different from that behind the body (corresponding to different values of ω for wing and body). This implies that the wake cross-section does not keep its shape and that the body vortex sheet moves downwards more rapidly

* Such plan-forms for swept wings by themselves have been derived by Küchemann in Ref. 8.

than that behind the wing. This, of course, cannot be taken into account completely in any theory, but we may make some allowance for it by increasing the downward velocity $v_{z\infty}$ (and thus the potential ϕ_2, equation (18)) for the body by the factor $2/\omega$. It is still reasonable to assume that the potential ϕ_1 is determined with sufficient accuracy by equation (17) from the original shape of the wake, since this is mainly due to the interference between the actual wing and body.

This leads to a change in the load coefficient given in equation (30) by

$$\frac{\Delta(C_L c)}{\bar{C}_{L\mathrm{W}}\bar{c}} = -\frac{\omega_\mathrm{B}-\omega}{\omega}\frac{4R/b}{J_\mathrm{W}}\sqrt{\left\{1-\left(\frac{y}{R}\right)^2\right\}}, \qquad \ldots\ldots\ldots\ldots \quad (38)$$

where $\omega_\mathrm{B} = 2$ in most cases, and to a change in the overall load on the body by

$$\frac{\Delta\bar{C}_{L\mathrm{B}}}{\alpha} = -\frac{\omega_\mathrm{B}-\omega}{\omega}\cdot\frac{2}{\omega}\frac{\alpha_i}{\alpha}\cdot 2\pi A\left(\frac{R}{b}\right)^2. \qquad \ldots\ldots\ldots\ldots \quad (39)$$

The load over the body calculated by equations (26), (30), (38) and (39) includes some of the load at the nose of the body. An approximation to the overall load on the body induced by the wing, excluding forces on the nose and the rear end of the body, is obtained by reducing the value given in equation (26) by

$$\frac{\Delta\bar{C}_{L\mathrm{B}}}{\alpha} = -\frac{v_{z\infty}}{V_0}\cdot 2\pi A\cdot\left(\frac{R}{b}\right)^2$$

$$= -\frac{2}{\omega}\frac{\alpha_i}{\alpha}\cdot 2\pi A\cdot\left(\frac{R}{b}\right)^2. \qquad \ldots\ldots\ldots\ldots \quad (40)$$

An approximation to the corresponding load distribution is obtained by reducing the value given by equation (30) by

$$\frac{\Delta C_{L\mathrm{B}}c}{\bar{C}_{L\mathrm{W}}\bar{c}} = -\frac{4R/b}{J_\mathrm{W}}\sqrt{1-\left(\frac{y}{R}\right)^2} \qquad \ldots\ldots\ldots\ldots \quad (41)$$

5. *The Limiting Case* $R \to 0$.—To show the effect of the body on the various terms and to facilitate the plotting of the diagrams, it is useful to consider the case of decreasing body diameter $R \to 0$. As $R \to 0$ the arrangement approaches a wing with elliptic load distribution. This follows from the above equations; when $R \to 0$: $\vartheta_2 \to 0$, $R_2 \to \frac{1}{4}b$, $\cos\vartheta \to 1 - y/\frac{1}{2}b$, $C_L c \to 2\frac{v_{z\infty}}{V_0}A\bar{c}\sqrt{\left\{1-\left(1-\frac{y}{b/2}\right)^2\right\}}$.

Then

$$\frac{\bar{C}_L}{\alpha} = \frac{\pi}{2}\cdot\frac{v_{z\infty}}{V_0}\cdot A, \quad \text{i.e., } J_\mathrm{W} = \frac{\pi}{2} \qquad \ldots\ldots\ldots\ldots \quad (42)$$

and

$$\frac{C_L c}{\bar{C}_L\bar{c}} = \frac{4}{\pi}\sqrt{\left\{1-\left(1-\frac{y}{b/2}\right)^2\right\}}. \qquad \ldots\ldots\ldots\ldots \quad (43)$$

When the sectional lift slope is constant along the span:

$$C_L = \bar{C}_L$$

which gives

$$a\left(1 - \frac{\omega}{2}\frac{v_{z\infty}/V_0}{\alpha}\right) = \frac{\pi}{2}\frac{v_{z\infty}/V_0}{\alpha}A$$

$$\frac{\alpha_i}{\alpha} = \frac{\omega}{2}\frac{v_{z\infty}/V_0}{\alpha} = \frac{\dfrac{\omega a}{2\pi A}}{\dfrac{1}{2} + \dfrac{\omega a}{2\pi A}} . \qquad \ldots \quad \ldots \quad \ldots \quad \ldots \quad (44)$$

To obtain the shape of the load distribution over the body for $R \to 0$, we expand $\sin\vartheta$ and $(1 - \cos\vartheta)$ as power series in ϑ and take only the first term:

$$\sin\vartheta = \vartheta$$

$$1 - \cos\vartheta = \frac{\vartheta^2}{2} .$$

Equations (14) and (15) then read:

$$y/R = \pm\sqrt{\left\{1 - \frac{4}{(\vartheta_2^2/2)^2}\frac{\vartheta^2}{2}\left(\frac{\vartheta_2^2}{2} - \frac{\vartheta^2}{2}\right)\right\}}$$

$$= 1 - 2\left(\frac{\vartheta}{\vartheta_2}\right)^2$$

$$\vartheta = \vartheta_2\sqrt{\left\{\frac{1 - y/R}{2}\right\}} .$$

Equation (21) becomes:

$$C_L c = 4\frac{v_{z\infty}}{V_0}\frac{4R}{1 - \cos\vartheta_2}\left[\vartheta - \frac{1 - \cos\vartheta_2}{4}\sqrt{\left\{1 - \left(\frac{y}{R}\right)^2\right\}}\right]$$

$$= 4\frac{v_{z\infty}}{V_0}\frac{8R}{\vartheta_2}\left[\sqrt{\left\{\frac{1 - y/R}{2}\right\}} - \frac{\vartheta_2}{8}\sqrt{\left\{1 - \left(\frac{y}{R}\right)^2\right\}}\right]$$

$$= 4\frac{v_{z\infty}}{V_0}\frac{8R}{\vartheta_2}\sqrt{\left\{\frac{1 - y/R}{2}\right\}}$$

since for $R \to 0$, i.e., $\vartheta_2 \to 0$, the second term in the bracket tends to zero. Since the load in the wing body junction is

$$C_{L\mathrm{j}} c_{\mathrm{j}} = 4\frac{v_{z\infty}}{V_0}\frac{8R}{\vartheta_2} ,$$

we have

$$\frac{C_L c}{C_{L\mathrm{j}}\, c_{\mathrm{j}}} = \sqrt{\left\{\frac{1 - y/R}{2}\right\}} . \qquad \ldots \quad \ldots \quad \ldots \quad \ldots \quad \ldots \quad (45)$$

The aerodynamic centre of this body load measured from the wing-body junction is

$$y_{\mathrm{a.c.}} = R\frac{\int_{-1}^{+1}\sqrt{\{1 - y/R\}}(1 + y/R)\, d(y/R)}{\int_{-1}^{+1}\sqrt{\{1 - y/R\}}\, d(y/R)} = 0{\cdot}8R .$$

6. *The Calculation Procedure.*—The known quantities for a given fin-body combination are: the aspect ratio A of the wing outside the body, the angle of sweep φ of the mid-chord line and the ratio between the body radius R and the wing span b. The first step is to determine the term $\omega a/2\pi A$. The sectional lift slope a and the downwash factor ω are calculated by the method of Ref. 7 as follows:—

The lift slope a_0 of the two-dimensional wing is approximately

$$a_0 = k \cdot 2\pi\left(1 + 0{\cdot}8\frac{t/c}{\cos\varphi_e}\right) \quad .. \quad .. \quad .. \quad .. \quad (46)$$

where t/c is the thickness/chord ratio; k is a factor for the lift reduction due to the boundary layer, which changes with Reynolds number ($k = 0{\cdot}92$ for R about 2×10^6). The value of the sectional lift slope a to be used here is given by

$$a = \frac{2a_0 n \cos\varphi_e}{1 - \pi n \cot \pi n} \quad .. \quad .. \quad .. \quad .. \quad .. \quad .. \quad (47)$$

where n is a parameter depending on the sweep and aspect ratio in the following way

$$n = 1 - \frac{1}{2\left\{1 + \left(\frac{a_0 \cos\varphi_e}{\pi A_e}\right)^2\right\}^{\frac{1}{4\left(1 + \left|\frac{\varphi_e}{\pi/2}\right|\right)}}} \quad .. \quad .. \quad .. \quad .. \quad (48)$$

The downwash factor ω is then

$$\omega = 2n \, . \quad .. \quad .. \quad .. \quad .. \quad .. \quad .. \quad (49)$$

For wings of small aspect ratio, the effective angle of sweep is smaller than the geometric sweep due to centre and tip effects. This can be taken into account by reducing the geometric sweep φ to

$$\varphi_e = \frac{\varphi}{\left\{1 + \left(\frac{a_0 \cos\varphi}{\pi A_e}\right)^2\right\}^{1/4}} \quad .. \quad .. \quad .. \quad .. \quad .. \quad (50)$$

and φ_e is the value to be inserted into equations (46), (47), (48).

The effective aspect ratio A_e which has to be taken in equations (48) and (50) varies between the aspect ratio A of the wing outside the body for $R/b \to 0$ and $2A$ for $R/b \to \infty$. A formula which satisfies the two limits is

$$A_e = A\left(1 + \frac{R/b}{1 + R/b}\right) \quad .. \quad .. \quad .. \quad .. \quad .. \quad (51)$$

which means that we take as the effective span b_e the distance between the wing tip $(b + R)$ and the image of the wing tip in the circle $R^2/(b + R)$ (*see* Fig. 8).

Using relations (46) to (50) the term $\omega a/2\pi A$ is calculated, and the induced incidence α_i/α for the given value of R/b is read from Fig. 7. The value of J_W for given R/b is then found from

Fig. 2 and the coefficient of the overall wing lift from

$$\frac{\bar{C}_{L\mathrm{W}}}{\alpha} = \frac{2}{\omega}\frac{\alpha_i}{\alpha} A J_{\mathrm{W}} . \qquad (52)$$

The ratio $\bar{C}_{L\mathrm{B}}/\bar{C}_{L\mathrm{W}}$ for constant induced downwash $\omega_{\mathrm{B}} = \omega$, is read from Fig. 3 and the overall lift coefficient, excluding the forces on the nose and rear end of the body, is

$$\frac{\bar{C}_L}{\alpha} = \frac{\bar{C}_{L\mathrm{W}}}{\alpha}\left(1 + \frac{\bar{C}_{L\mathrm{B}}}{\bar{C}_{L\mathrm{W}}}\right) - \frac{2}{\omega}\frac{\alpha_i}{\alpha} 2\pi A \left(\frac{R}{b}\right)^2 . \qquad (53)$$

The spanwise load distribution is obtained from

$$\frac{C_L c}{\alpha \bar{c}} = \frac{\bar{C}_{L\mathrm{W}}}{\alpha} \cdot \frac{C_L c}{\bar{C}_{L\mathrm{W}} \bar{c}} \quad \text{for the wing} \qquad (54)$$

and

$$\frac{C_L c}{\alpha \bar{c}} = \frac{\bar{C}_{L\mathrm{W}}}{\alpha}\left(\frac{C_L c}{\bar{C}_{L\mathrm{W}} \bar{c}} - \frac{4R/b}{J_{\mathrm{W}}}\sqrt{1 - \left(\frac{y}{R}\right)^2}\right) \quad \text{for the body} \qquad (55)$$

where $C_L c/\bar{C}_{L\mathrm{W}}\bar{c}$ is read off Figs. 4, 5 and 6 for the appropriate values of R/b.

Although in practice the plan-form will be different from that which gives constant downwash, the results can be applied to wings of any plan-form. A rough approximation for the lift distribution on the actual wing-body arrangement is obtained by dividing the calculated load distribution equation (54) by the actual $c(y)/\bar{c}$ values.

To obtain a better approximation the differences between the local loads with body and without body are taken

$$\frac{\Delta C_L c}{\bar{c}} = \bar{C}_{L\mathrm{W}} \cdot \frac{C_L c}{\bar{C}_{L\mathrm{W}} \bar{c}} - \bar{C}_{L\mathrm{E}} \frac{4}{\pi}\sqrt{1 - \left(1 - \frac{y}{b/2}\right)^2} \qquad (56)$$

where $\bar{C}_{L\mathrm{E}}$ is the lift of the elliptic wing alone:

$$\frac{\bar{C}_{L\mathrm{E}}}{\alpha} = \frac{2}{\omega}\frac{\alpha_{i\mathrm{E}}}{\alpha} A \frac{\pi}{2} . \qquad (57)$$

The induced incidence $\alpha_{i\mathrm{E}}/\alpha$ can be determined from Fig. 7 for $R = 0$ when a and ω have been calculated from equations (46) to (50) for the given A and φ. This $\Delta C_L/\alpha$ distribution is added to the C_L/α distribution of the actual wing without body, which can be calculated by the usual methods. This procedure has been satisfactorily applied to wings with endplates, *see* Ref. 5.

The wing alone and the wing with body, both giving constant downwash, do not have the same plan-form, so that a better approximation for the ΔC_L distribution is obtained by calculating from equation (34) the plan-form of the wing which in the presence of the body gives constant down wash, and calculating the load distribution of that wing without a body. This gives the exact effect of the body on the load distribution of a certain wing. In this way, different values of the sectional lift slope a along the span can be taken into account. In practice, this refinement

alters the results very little, as has been shown in Ref. 4. It is essential, however, to use variable values of a in the calculation of the distribution on the wing alone.

7. *The Induced Drag.*—Considering the change of energy and momentum of the flow far upstream and in the wake, we obtain for constant downwash along the span, $\omega_B = \omega$, the well-known relation between the induced drag and the lift coefficient

$$\bar{C}_{Di} = \frac{1}{2}\frac{v_{z\infty}}{V_0}\bar{C}_L . \qquad (58)$$

With

$$\bar{C}_L = \frac{v_{z\infty}}{V_0} A J_W \left(1 + \frac{\bar{C}_{LB}}{\bar{C}_{LW}}\right)$$

we obtain

$$\bar{C}_{Di} = \frac{\bar{C}_L^2}{\pi A} \frac{\pi}{2J_W\left(1 + \frac{\bar{C}_{LB}}{\bar{C}_{LW}}\right)} . \qquad (59)$$

Introducing the notation

$$\bar{C}_{Di} = \varkappa . \frac{\bar{C}_L^2}{\pi A} \qquad (60)$$

(as is done in the theory of end plates) we can find $\varkappa$ from the values of J_W and $\bar{C}_{LB}/\bar{C}_{LW}$ in Figs. 2 and 3. Values of $\varkappa$, which depend only on the ratio R/b, are plotted in Fig. 9.

It may be noted that one cannot determine an equivalent end-plate for a body attached to a wing. The lift distribution and thus the vortex-system are different for a wing with endplate and a wing with body, since the body can take a lift force, which vertical endplates cannot do. With increasing ratio R/b, the lift distribution over the wing does not tend to the half-ellipse as it does for increasing height of the endplate.

LIST OF SYMBOLS

x,y,z		Rectangular system of co-ordinates, x in the wind direction, y spanwise, z positive downwards ; origin on the body axis
ζ	=	$z + iy$, complex co-ordinate in the Trefftz-plane
ζ_1	=	$z_1 + iy_1$, co-ordinate in the transformed Trefftz-plane, where the body cross-section is transformed into a vertical end-plate
ζ_2	=	$z_2 + iy_2$, co-ordinate in the transformed Trefftz-plane, where the wake contour is transformed into a circle
ϑ		Angular co-ordinate in the ζ_2-plane
ϑ_1		ϑ-value of the point corresponding to the top of the body
ϑ_2		ϑ-value of the point corresponding to the wing body junction
c		Local wing chord
$\bar{c}$		Mean chord of the wing outside the body

b Wing span

b_1 Wing span in the ζ_1-plane

R Body radius

h Height of the end-plate in the ζ_1-plane

R_2 Radius of the circle into which the wake contour is transformed in the ζ_2-plane

$A = \frac{b}{\bar{c}}$, aspect ratio of the wing outside the body

φ Angle of sweep of the mid-chord line

φ_e Effective angle of sweep, *see* equation (50)

α Geometric incidence

$\Delta\alpha_B$ Additional upwash produced by the flow around the isolated body

α_i Induced angle of incidence

V_0 Velocity of the main flow

$v_{z\infty}$ Downwash velocity in the Trefftz-plane

ϕ Potential

C_L Local lift coefficient

$\bar{C}_{LW}$ Coefficient of the overall lift on the wing

$\bar{C}_{LB}$ Coefficient of the overall lift on the body referred to the wing area $b\bar{c}$

$\bar{C}_L = \bar{C}_{LW} + \bar{C}_{LB}$, overall lift coefficient referred to the wing area $b\bar{c}$

$\bar{C}_{Di}$ Coefficient of the overall induced drag referred to the wing area $b\bar{c}$

$a = \frac{dC_L}{d\alpha_{eff}}$, local sectional lift slope

a_0 Lift slope coefficient of the two-dimensional aerofoil

$\omega = \frac{\alpha_i}{\frac{v_{z\infty}/V_0}{2}}$ Downwash factor

ω_B Downwash factor for the body

$J_W = \frac{\bar{C}_{LW}}{A \,.\, v_{z\infty}/V_0}$

Suffices:

$_W$ Wing

$_B$ Body

$_j$ Junction

$_e$ Effective

$_E$ Elliptic wing alone

REFERENCES

No.	*Author*	*Title, etc.*
1	W. Mangler	The distribution of lift over an aerofoil with end-plates. *L.F.F.*, Vol. 14, p. 564. 1938. Translated as A.R.C. 3414.
2	J. Rotta	Luftkräfte am Tragflügel mit einer seitlichen Scheibe. *Ing. Archive*, Vol. 13, p. 119. 1942.
3	W. Mangler and J. Rotta	Theory of three-dimensional aerofoils. Section 1.6: Aerofoils with tip plates. Ministry of Supply R. & T. 1023. 1947.
4	D. E. Hartley	Theoretical load distributions on wings with tip-tanks. C.P. 147. January, 1952.
5	D. Küchemann and D. J. Kettle ..	The effect of end-plates on swept wings. C.P.104. June, 1951.
6	J. Weber, D. A. Kirby and D. J. Kettle	An extension of Multhopp's method of calculating the spanwise loading of wing-fuselage combinations. R. & M. 2872. November, 1951.
7	D. Küchemann	A simple method for calculating the span- and chordwise loading on straight and swept wings of any given aspect ratio at subsonic speeds. R. & M. 2935. August, 1952.
8	D. Küchemann	A simple method for calculating the span- and chordwise loadings on thin swept wings. R.A.E. Report Aero. 2392. A.R.C. 13,758. August, 1950.

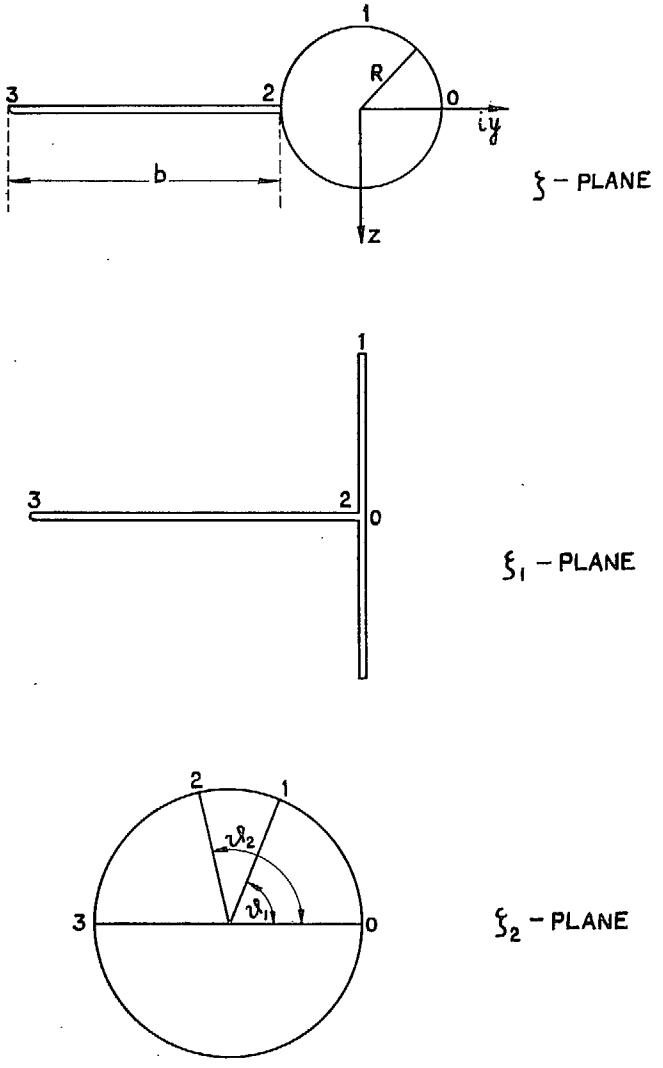

FIG. 1. Transformations of the Trefftz-plane.

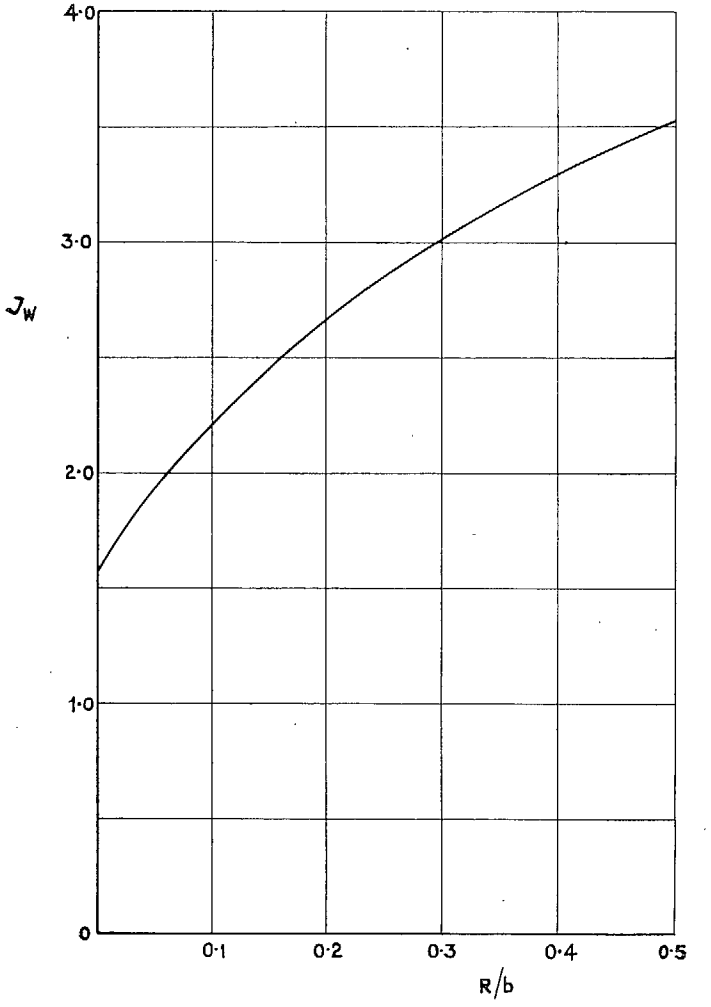

FIG. 2. Coefficient for calculating the wing lift. $\bar{C}_{LW}/\alpha = J_W \cdot A \cdot 2/\omega \cdot \alpha_i/\alpha$.

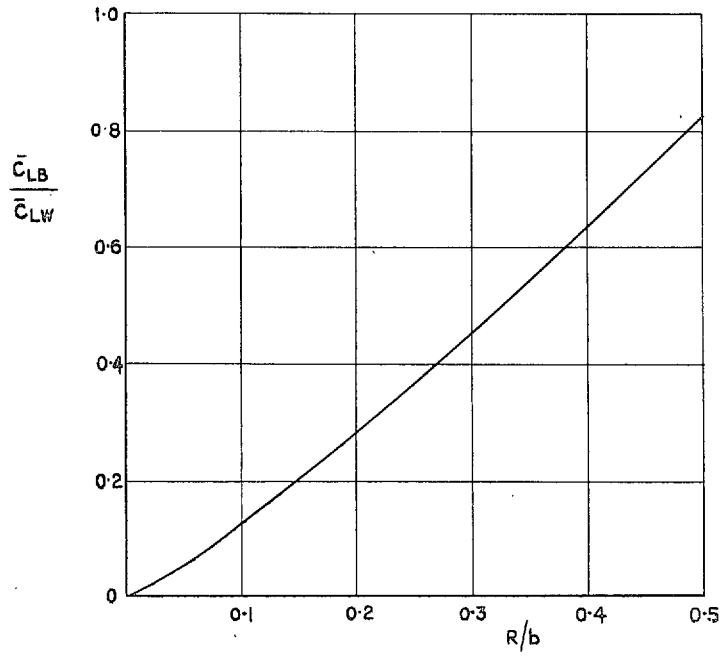

FIG. 3. Ratio between body lift and wing lift for $\omega_B = \omega$.

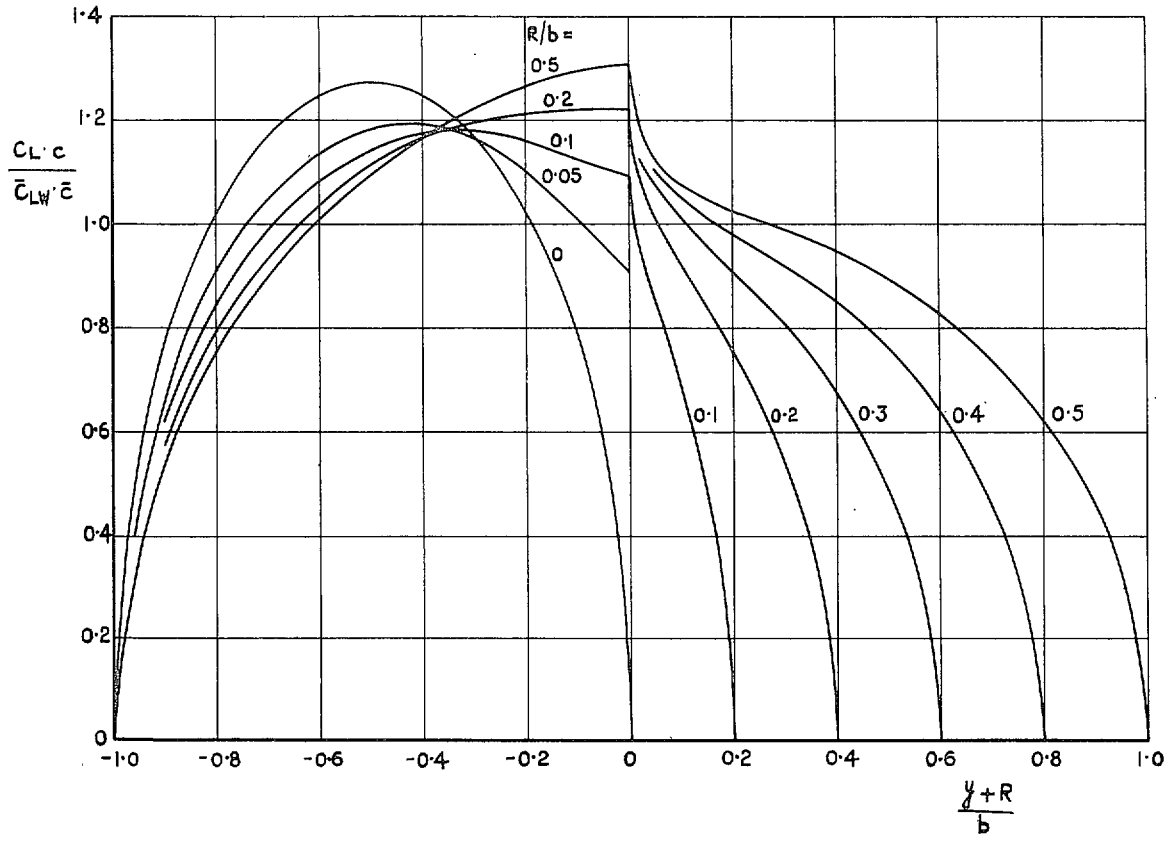

FIG. 4. Spanwise load distributions for $\omega_B = \omega$.

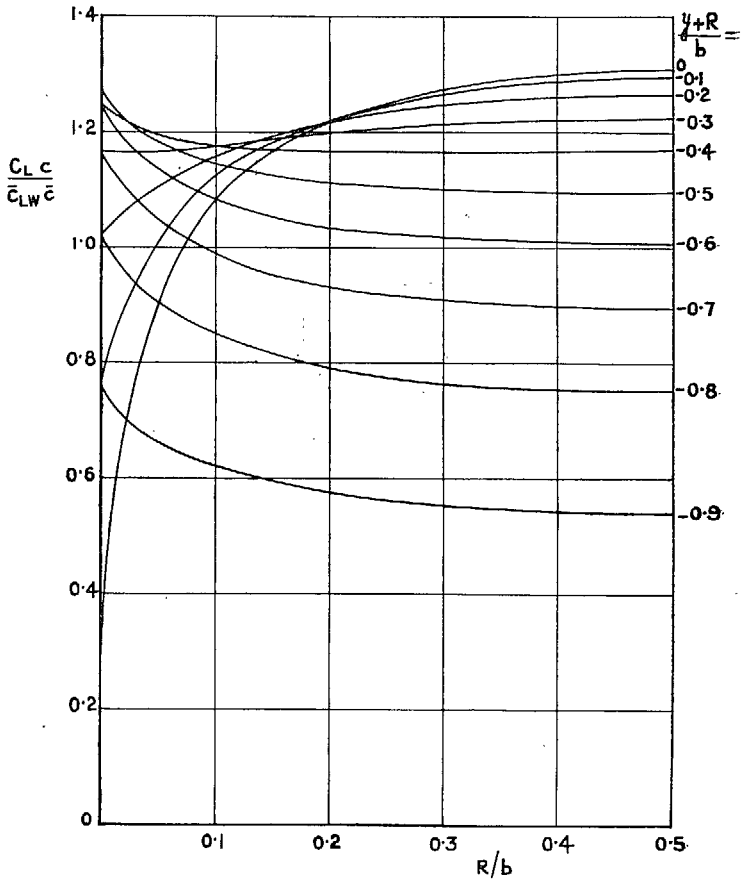

FIG. 5. Load coefficient on the wing.

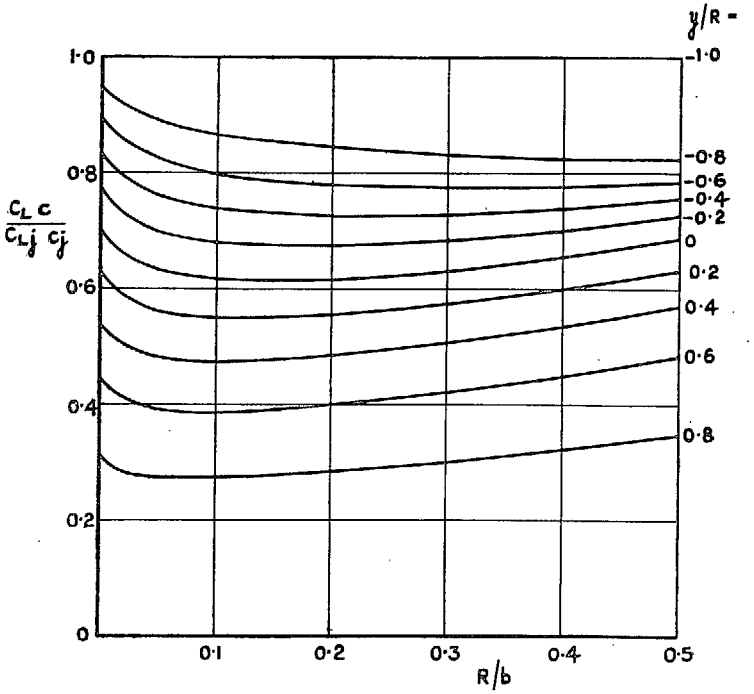

FIG. 6. Load coefficient across the body for $\omega_B = \omega$.

(6934) Wt. 18/680 K.7 11/57 H.P.Co. 34-261

PRINTED IN GREAT BRITAIN

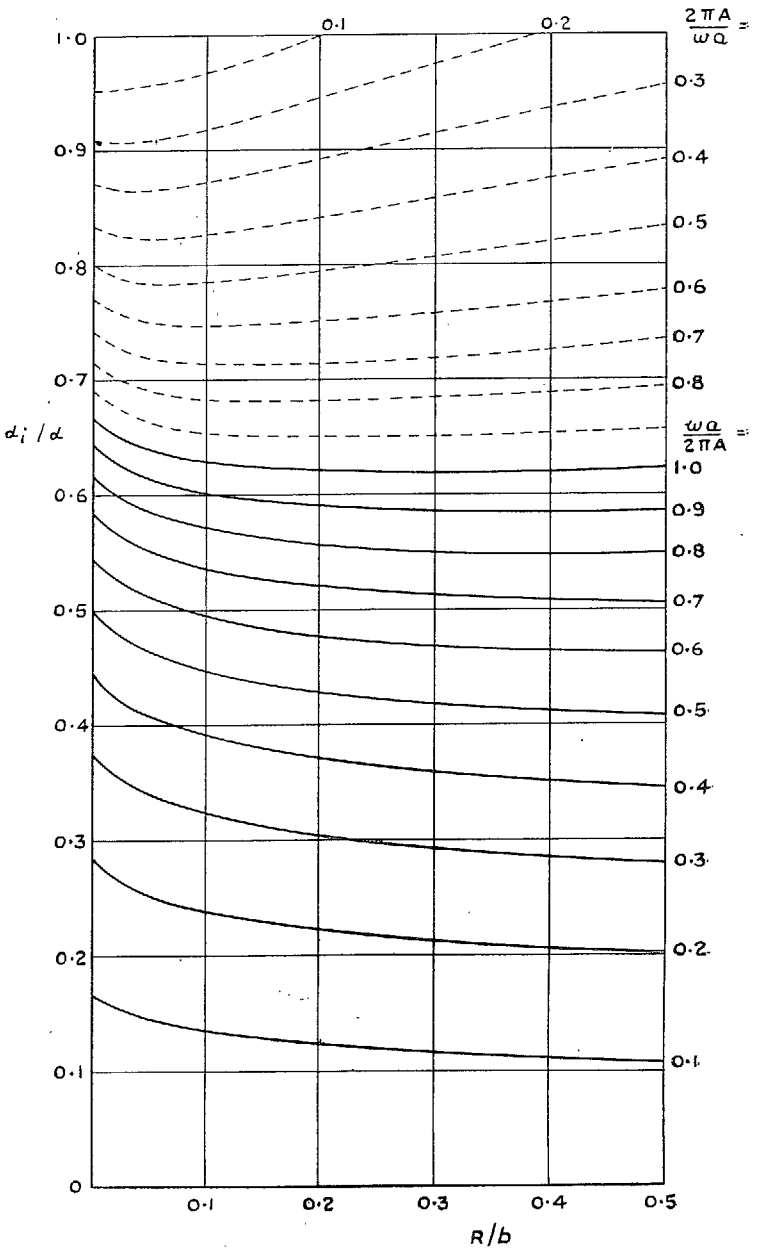

FIG. 7. Induced incidence.

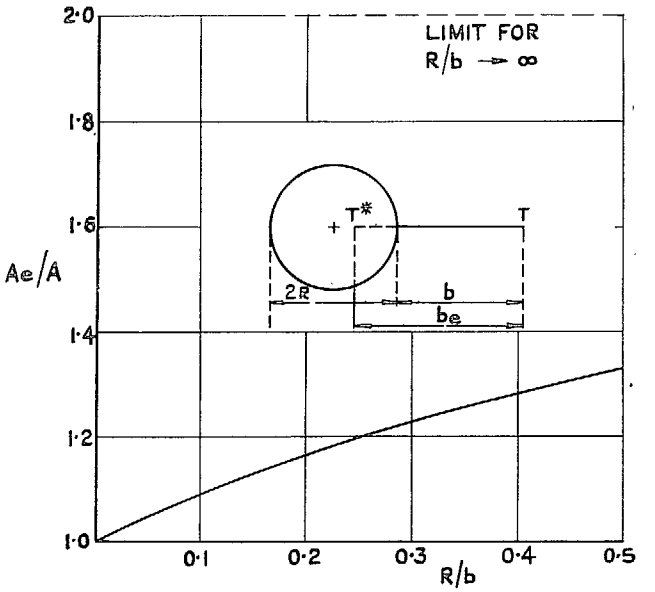

FIG. 8. Effective aspect ratio.

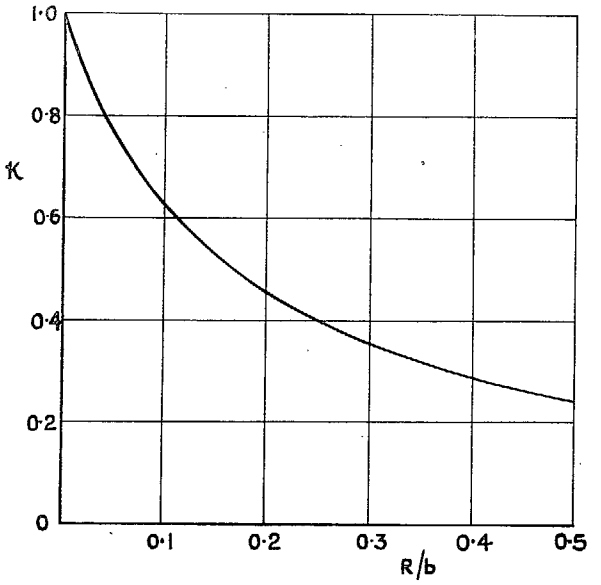

FIG. 9. Induced drag reduction. $\bar{C}_{Di} = \varkappa \bar{C}_L^2 / \pi A$.

Publications of the Aeronautical Research Council

ANNUAL TECHNICAL REPORTS OF THE AERONAUTICAL RESEARCH COUNCIL (BOUND VOLUMES)—

1939 Vol. I. Aerodynamics General, Performance, Airscrews, Engines. 50*s.* (52*s.*)
Vol. II. Stability and Control, Flutter and Vibration, Instruments, Structures, Seaplanes, etc. 63*s.* (65*s.*)

1940 Aero and Hydrodynamics, Aerofoils, Airscrews, Engines, Flutter, Icing, Stability and Control, Structures, and a miscellaneous section. 50*s.* (52*s.*)

1941 Aero and Hydrodynamics, Aerofoils, Airscrews, Engines, Flutter, Stability and Control, Structures. 63*s.* (65*s.*)

1942 Vol. I. Aero and Hydrodynamics, Aerofoils, Airscrews, Engines. 75*s.* (77*s.*)
Vol. II. Noise, Parachutes, Stability and Control, Structures, Vibration, Wind Tunnels. 47*s.* 6*d.* (49*s.* 6*d.*)

1943 Vol. I. Aerodynamics, Aerofoils, Airscrews. 80*s.* (82*s.*)
Vol. II. Engines, Flutter, Materials, Parachutes, Performance, Stability and Control, Structures. 90*s.* (92*s.* 9*d.*)

1944 Vol. I. Aero and Hydrodynamics, Aerofoils, Aircraft, Airscrews, Controls. 84*s.* (86*s.* 6*d.*)
Vol. II. Flutter and Vibration, Materials, Miscellaneous, Navigation, Parachutes, Performance, Plates and Panels, Stability, Structures, Test Equipment, Wind Tunnels. 84*s.* (86*s.* 6*d.*)

1945 Vol. I. Aero and Hydrodynamics, Aerofoils. 130*s.* (132*s.* 9*d.*)
Vol. II. Aircraft, Airscrews, Controls. 130*s.* (132*s.* 9*d.*)
Vol. III. Flutter and Vibration, Instruments, Miscellaneous, Parachutes, Plates and Panels, Propulsion. 130*s.* (132*s.* 6*d.*)
Vol. IV. Stability, Structures, Wind Tunnels, Wind Tunnel Technique. 130*s.* (132*s.* 6*d.*)

ANNUAL REPORTS OF THE AERONAUTICAL RESEARCH COUNCIL—

1937 2*s.* (2*s.* 2*d.*) 1938 1*s.* 6*d.* (1*s.* 8*d.*) 1939–48 3*s.* (3*s.* 5*d.*)

INDEX TO ALL REPORTS AND MEMORANDA PUBLISHED IN THE ANNUAL TECHNICAL REPORTS, AND SEPARATELY—

April, 1950 . . . . . R. & M. No. 2600 2*s.* 6*d.* (2*s.* 10*d.*)

AUTHOR INDEX TO ALL REPORTS AND MEMORANDA OF THE AERONAUTICAL RESEARCH COUNCIL—

1909–January, 1954 . . . R. & M. No. 2570 15*s.* (15*s.* 8*d.*)

INDEXES TO THE TECHNICAL REPORTS OF THE AERONAUTICAL RESEARCH COUNCIL—

December 1, 1936 — June 30, 1939	R. & M. No. 1850	1*s.* 3*d.* (1*s.* 5*d.*)
July 1, 1939 — June 30, 1945	R. & M. No. 1950	1*s.* (1*s.* 2*d.*)
July 1, 1945 — June 30, 1946	R. & M. No. 2050	1*s.* (1*s.* 2*d.*)
July 1, 1946 — December 31, 1946	R. & M. No. 2150	1*s.* 3*d.* (1*s.* 5*d.*)
January 1, 1947 — June 30, 1947	R. & M. No. 2250	1*s.* 3*d.* (1*s.* 5*d.*)

PUBLISHED REPORTS AND MEMORANDA OF THE AERONAUTICAL RESEARCH COUNCIL—

Between Nos. 2251–2349	R. & M. No. 2350	1*s.* 9*d.* (1*s.* 11*d.*)
Between Nos. 2351–2449	R. & M. No. 2450	2*s.* (2*s.* 2*d.*)
Between Nos. 2451–2549	R. & M. No. 2550	2*s.* 6*d.* (2*s.* 10*d.*)
Between Nos. 2551–2649	R. & M. No. 2650	2*s.* 6*d.* (2*s.* 10*d.*)

Prices in brackets include postage

HER MAJESTY'S STATIONERY OFFICE

York House, Kingsway, London, W.C.2; 423 Oxford Street, London, W.1; 13a Castle Street, Edinburgh 2; 39 King Street, Manchester 2; 2 Edmund Street, Birmingham 3; 109 St. Mary Street, Cardiff; Tower Lane, Bristol 1; 80 Chichester Street, Belfast *or through any bookseller.*

S.O. Code No. 23–2889